Feature augmentation for numerical inversion of multi-exponential decay curves

Feature augmentation for numerical inversion of multi-exponential decay curves

Rosanna Campagna[1,a)] and Emma Perracchione[2,b)]

[1]*Department of Mathematics and Physics, University of Campania "Luigi Vanvitelli", Caserta, Italy*
[2]*Department of Mathematics DIMA, University of Genova, Genova, Italy*

[a)]Corresponding author: rosanna.campagna@unicampania.it
[b)]perracchione@dima.unige.it

Abstract. Multi-exponential decay curves describe the nuclear magnetic resonance response to radiofrequency exposure. This problem is strongly related to finding a non-negative function given a finite number of noisy values of its Laplace Transform. The solution of this inverse problem takes advantage from a functional modelling of the data. We propose a fitting procedure based on the definition of a meshfree interpolant computed via a variably scaled kernel strategy. A parametric weighted sum of a finite number of exponential terms is introduced to describe the data behaviour; a data-driven procedure estimates its free parameters to scale the kernel, acting as a feature augmentation strategy. The performances of this procedure are investigated on real data sets from nuclear magnetic resonance acquisitions in the context of food science.

Introduction

Most of empirical experiments in natural sciences are *discrete indirect*. Indeed, starting from a sampling of a time-dependent function s, the target function g is computed by solving an inverse problem. We focus on the following:

Problem 1 *Given* (t_i, s_i)*,* $i = 1, \dots, N$*, a finite set of* noisy *data,*

$$s_i = s(t_i) + \varepsilon_i, \quad i = 1, \dots, N,$$

with ε_i*,* $i = 1, \dots, N$*, from unknown noise sources, compute the* inverse *function* g *under the hypothesis on the unknown* s*:*

$$s(t) = \int_a^b K(t, \tau) g(\tau) d\tau, \quad a, b, t \in \mathbb{R}^+. \tag{1}$$

For most kernels, estimating g results an *ill-posed* problem, e.g. if $K(t, \tau) = e^{-t\tau}$ such issue is referred to as *discrete Laplace Transform (LT) inversion* problem. Nuclear Magnetic Resonance (NMR) relaxometry is strongly linked to the numerical inversion of the LT of a non-negative function, where the NMR signal s is measured at different times $t_1, \dots, t_n$, and it is related to the distribution density g of the NMR relaxation times by (1).

NMR occurs when the nuclei of certain atoms are immersed in a static magnetic field and exposed to radio frequency waves. The nuclei recognize this phenomenon depending on their spin property. A growing interest of this technique in the context of food technologies is confirmed by studies concerning the use of low-resolution proton NMR, to measure the transverse relaxation times in dough and bread (see e.g. [1]). More recently, the NMR analysis has been applied to investigate the water mobility in the dough during the mixing phase of the breadmaking process, due to the interactions of the flour polymers with water [2]; in recent years, low-resolution 1H NMR turned out to be a useful tool to study how water-polymers interactions change in food matrices, such as e.g. the pasta, as function of composition [3] as well as of process parameters. By discretizing the functional (1) we describe the magnetization function s as a sum of exponentially decaying components:

$$s(t) = \sum_{j=1}^{M} g_j e^{-t\tau_j}, \tag{2}$$

where $g_j \geq 0$, $\tau_j > 0$, $j = 1, \ldots, M$, t is the experimental time, M is the number of micro-domains having the same spin density and g_j are the amplitudes of the corresponding relaxation time distribution. The number of exponential components M can range from 1 to larger numbers; however, in practice, the sum is assumed on two or at most three terms. The relaxation function s is normalized to unity, it is always positive, and monotonically decreases to zero for any time $t > 0$. In [4] several methods, both deterministic and stochastic, are compared to solve the nuclear magnetic resonance relaxometry problem, assumed that it can be traced to a LT inversion problem. In [2] the solution is computed by solving a constrained minimization problem:

$$\min_{\mathbf{g}} \ \|\mathbf{s} - A\mathbf{g}\|^2 + \lambda^2 \|L\mathbf{g}\|^2 \qquad s.t. \qquad \begin{cases} g_j \geq 0, \quad j = 2, \ldots, M-1 \\ g_1 = 0, \ g_M = 0 \end{cases} \tag{3}$$

where $\|\cdot\|$ is the Euclidean norm, $\mathbf{s}$ is the data vector, A is the matrix obtained from the discretization of the integral in (1), $\mathbf{g}$ is the discrete solution, λ is a regularization parameter and L is the discrete Laplace operator, defined as $(L\mathbf{g})_i = 2g_i - g_{i-1} - g_{i+1}$. In the experiments we set $\lambda = 10^{-2}$. The numerical solution often requires precise data distributions and this hypothesis is *not always* satisfied in the applications. The relaxation decay curves can be fitted with classical polynomial or spline models [5, 6]. The noisy nature of the data encourages the use of smooth models, preserving from noise amplification deriving from the interpolating constraints. Here we propose a Variably Scaled Kernel (VSK) model [7]. The definition of VSKs relies upon a scaling function which is introduced as a feature augmentation strategy. To extract information from the data appropriately, the scaling function is defined as a parametric weighted sum of a finite number of exponential terms, whose parameters are deduced by a non-linear fitting of the samples. This novel VSK model is introduced to overcome some issues common to many approximating models. Indeed, the computational cost of these models strongly depends on the knots, when they are identified with the data. Nevertheless, only a reduce number of data can be assumed sufficient to capture their trend. With these considerations in mind, we show how our approach can help to describe the global trend starting from *any* (also randomly selected) subset of data. The so-defined functional description of the multi-exponential decay data can be a useful pre-processing stage for the application of any LT inversion method, generally based on the collocation and evaluation of the LT function, as a wide literature confirms (see, e.g. [8, 9, 10, 11, 12, 13]).

RBF-VSK feature augmentation results for NMR

The data set used in the following experiments derives from a real problem where the effects of the NMR on the changes in water molecule mobility during the mixing phase of the bread making process are studied (for further details see e.g. [2]). The data distribution follows a multiexponential decay of the signal and consists of $N = 200$ mean values of three different acquisitions of transverse relaxation times for water protons in flour doughs, at mixing time of 3 minutes long. Given those data, i.e. $\{(t_i, s_i),\ i = 1, \ldots, N\} \subseteq \Omega \times \mathbb{R}^+$, $\Omega \subset \mathbb{R}^+$ as in Problem 1, we first model such samples via our kernel-based method and then we compute the inverse LT of such smooth model. We remark that a Radial Basis Function (RBF)-based model $P_s : \Omega \longrightarrow \mathbb{R}$ that interpolates such data assumes the form

$$P_s(t) = \sum_{k=0}^{N} a_k \phi(\|t - t_k\|), \quad t \in \Omega,$$

where ϕ is the so-called RBF and $\|\cdot\|$ is the Euclidean norm. The coefficients are characterized by solving the linear system of equations $K\boldsymbol{a} = \boldsymbol{s}$, where $\boldsymbol{a} = (a_0, \ldots, a_N)^\intercal$, $\boldsymbol{s} = (s_0, \ldots, s_N)^\intercal$ and $K_{ik} = \phi(\|t_i - t_k\|)$, $i, k = 0, \ldots, N$; see e.g. [14] for further details. In the varying scale setting, see e.g. [7], we define a *scaling* function $\psi : \Omega \longrightarrow \mathbb{R}$ and the RBF-VSK interpolant $P_s^\psi : \Omega \longrightarrow \mathbb{R}$ reads as follows

$$P_s^\psi(t) = \sum_{k=1}^{N} a_k^\psi K^\psi(t, t_k) = \sum_{k=1}^{N} a_k^\psi K((t, \psi(t)), (t, \psi(t_k))) = P_s((t, \psi(t)), \quad t \in \Omega.$$

Since the function ψ maps the original set of data, this step can be seen as a feature augmentation strategy. The definition of the scale function plays a crucial role and it might be selected so that it *mimics* the samples [15, 16, 17]. We then select it by taking a non-linear fit of the data considering a parametric sum of $M = 2$ exponentials as in (2). Moreover, in the following experiments we fix the Thin Plate Spline as RBF basis and we also investigate the construction of a reduced model on n samples with $n \ll N$ to smooth out the noise. We now focus on the performances

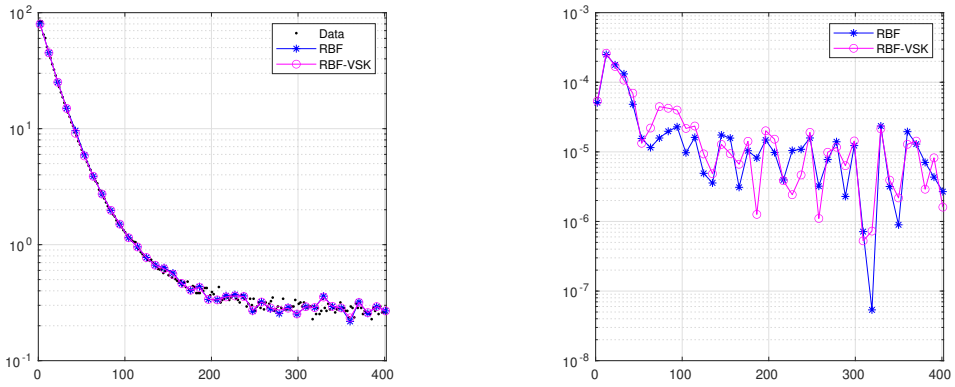

Figure 1. Left: fitting of 100 randomly selected data. Right: residuals computed as in (4). The black dots represent the real data, the blue stars the results obtained via classical RBFs and the magenta circle the ones computed via RBF-VSKs.

of the RBF-VSK fitting model for the considered NMR data set. The effects of the fitting errors introduced by our model are considered on the relaxation times distribution of the sampled signal s. To estimate them we report the pointwise residuals on the computed solution. Computationally speaking we use the MATLAB® function `rilt.m` available at the Mathworks File Exchange, that implements a Regularized Inverse Laplace Transform algorithm based on weighted least squares solution of (3) (see [18]). The *best* fitting parameters used to define the function ψ are estimated by the Matlab function `fminsearch` that uses the Nelder-Mead simplex algorithm [19]. Being real and noisy data the approximation might suffer from instability. To partially overcome this drawback, we introduce a Tikhonov parameter to avoid the matrix inversion; refer to [14]. Nevertheless, as we will point out, this might not be effective enough and therefore, reducing the number of data is recommended. To accomplish this, we perform two different strategies: (a) randomly select $n \ll N$ points, (b) select the first $n \ll N$ data and then extrapolate on the reconstruction interval. We expect that with both strategies the noise on the smoothed reconstruction will be sensibly reduced. However, note that the extrapolation issue mentioned in the second item is a challenging and ill-conditioned problem for which the VSKs turn out to be necessary. Indeed, referring to the left frames of Figures 1 and 2, fixed $n = 100$, we note that:

(a) with $n \ll N$ randomly selected data both RBF and RBF-VSK perform similarly, meaning that none of the two methods is able to truly smooth out the noise;
(b) with the first $n \ll N$ data, the RBF method fails in the extrapolation, while the RBF-VSK, taking advantage of the augmented feature, produces accurate and smooth approximations.

The considerations made above on the curve fitting are further supported by the solution of the inverse problem. Indeed, in the right frame of Figures 1 and 2, we report the residuals at the last step of the iterative algorithm by solving (3), where we take $n_{\text{eval}} = 60$ equispaced evaluation points $\tilde{\boldsymbol{x}}_i$, $i = 1, \ldots, n_{\text{eval}}$:

$$r_i = \frac{P_s(\tilde{\boldsymbol{x}}_i) - Ag_i}{n_{\text{eval}}}. \tag{4}$$

Discussion and work in progress

From the NMR example, we note that only the RBF-VSK model extrapolating on the last 100 nodes is able to provide a smooth approximation of the inverse problem. Moreover, for inversion issue it turns out to be somehow computationally less expensive than classical RBF approximation. Indeed, let m be the number of iterations that the method used for computing the inverse LT needs to converge. Concerning the computational efficiency of the proposed method, we have that in the framework of Figure 1, $m = 100$ and 18 for RBF and RBF-VSK, respectively. Analogously, in the framework of Figure 2, we obtain $m = 23$ and 19 for RBF and RBF-VSK, respectively.

As future work, we need to investigate suitable techniques to better select the collocation points. In this direction, we have to study the use of the so-called *greedy* methods [20, 21].

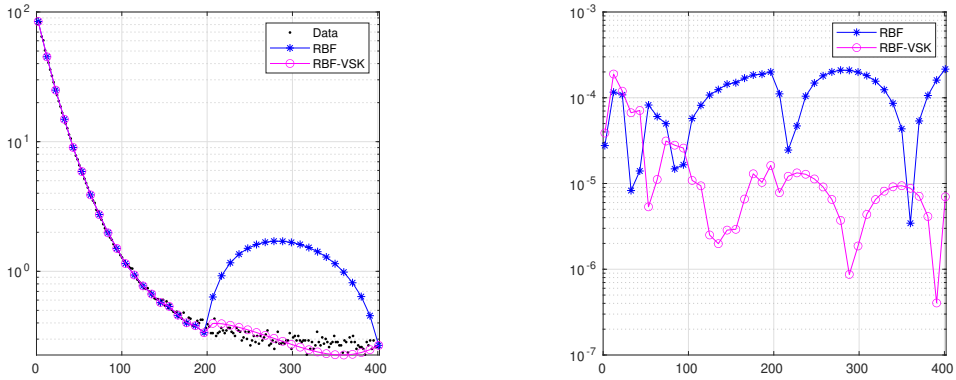

Figure 2. Left: fitting of the first 100 data. Right: residuals computed as in (4). The black dots represent the real data, the blue stars the results obtained via classical RBFs and the magenta circle the ones computed via RBF-VSKs.

Acknowledgments

We thank Prof. P. Masi (Dept. of Agricultural Sciences, University of Naples Federico II, Italy) and his group for sharing the NMR dataset and for the useful discussions on the problem. This research has been accomplished within Rete ITaliana di Approssimazione (RITA), partially funded by GNCS-INδAM.

References

[1] G. M. Bosmans, B. Lagrain, L. J. Deleu, E. Fierens, B. P. Hills, and J. A. Delcour, J. Agric. Food Chem. **60**, 5461–5470 (2012).

[2] A. Romano, R. Campagna, P. Masi, and G. Toraldo, "NMR data analysis of water mobility in wheat flour dough: A computational approach," in *Numerical Computations: Theory and Algorithms*, edited by Y. D. Sergeyev and D. E. Kvasov (Springer International Publishing, Cham, 2020), pp. 146–157.

[3] V. Gallo, A. Romano, and P. Masi, Food Struct. **24**, p. 100139 (2020).

[4] P. Barone, A. Ramponi, and G. Sebastiani, Inverse Probl. **17**, 77–94jan (2001).

[5] R. Campagna, C. Conti, and S. Cuomo, Dolomites Res. Notes Approx. **12**, 86–100 (2019).

[6] L. D'Amore, R. Campagna, A. Galletti, L. Marcellino, and A. Murli, Inverse Probl. **28**, p. 025007jan (2012).

[7] M. Bozzini, L. Lenarduzzi, M. Rossini, and R. Schaback, IMA J. Numer. Anal. **35**, 199–219 (2015).

[8] L. D'Amore, V. Mele, and R. Campagna, Inverse Probl. Sci. En. **26**, 553–580 (2018).

[9] S. Cuomo, L. D'Amore, and A. Murli, J. Comput. Appl. Math. **210**, 149–158 (2007), proceedings of the Numerical Analysis Conference 2005.

[10] L. D'Amore, R. Campagna, V. Mele, and A. Murli, Numer. Algorithms **63**, 187–211 (2013).

[11] L. D'Amore, R. Campagna, V. Mele, and A. Murli, ACM Trans. Math. Softw. **40**, 31:1–31:20 (2014).

[12] S. Cuomo, L. D'Amore, A. Murli, and M. Rizzardi, J. Comput. Appl. Math. **198**, 98–115January (2007).

[13] R. Campagna, C. Conti, and S. Cuomo, Appl. Math. Comput. **383**, p. 125376 (2020).

[14] G. E. Fasshauer, *Meshfree Approximation Methods with MATLAB*, Interdisciplinary mathematical sciences (World Scientific, Singapore, 2007).

[15] S. De Marchi, W. Erb, F. Marchetti, E. Perracchione, and M. Rossini, SIAM J. Sci. Comput. **42**, B472–B491 (2020).

[16] S. De Marchi, F. Marchetti, and E. Perracchione, BIT Numer. Math. **60**, 441–463 (2020).

[17] L. Romani, M. Rossini, and D. Schenone, J. Comput. Appl. Math. **349**, 532 – 547 (2019).

[18] S. W. Provencher, Comput. Phys. Commun. **27**, 213 – 227 (1982).

[19] J. C. Lagarias, J. A. Reeds, M. H. Wright, and P. E. Wright, SIAM J. Optimiz. **9**, 112–147 (1998).

[20] G. Santin and B. Haasdonk, Dolomites Res. Notes Approx. **10**, 68–78 (2017).

[21] D. Wirtz and B. Haasdonk, Dolomites Res. Notes Approx. **6**, 83–100 (2013).